Computational Research Progress in Applied Science & Engineering

ISSN 2423-4591

CRPASE Vol. 04(03), 55-61, October 2018

Performance Evaluation of Semi-Active Vehicle Suspension System Utilizing a New Adaptive Neuro-Fuzzy Controller Associated with Wavelet Transform

Abbas Soltani[a*], Shahram Azadi[b], Seung-Bok Choi[c], Ahmad Bagheri[a]

[a] *Department of Mechanical Engineering, University of Guilan, Rasht, Iran*
[b] *Department of Mechanical Engineering, K.N. Toosi of Technical University, Tehran, Iran*
[c] *Smart Structures and Systems Laboratory, Department of Mechanical Engineering, Inha University, Incheon, South Korea*

Keywords

Semi-active vehicle,
MR damper,
ANFIS controller,
Wavelet transform,
Power spectral density.

Abstract

In this paper, a magneto-rheological (MR) damper-based semi-active vehicle suspension is proposed using a new adaptive neuro-fuzzy inference system (ANFIS) controller associated with the wavelet transform (WT). A quarter-car suspension model is adopted for the controller design. When the resonance phenomena occurs on vertical wheel motion, the semi-active suspension system (SASS) based on ANFIS with constant gains cannot be very effective. In order to overcome this difficulty, the scaling factor of ANFIS is tuned by power spectral density (PSD) and WT methods. Simulation results on the random road input with highly transient phenomena show that the WT is more proper compared to the PSD method for analyzing the signals including transient characteristics and improving SASS performance.

1. Introduction

The main duty of a vehicle suspension system is to improve ride comfort, via attenuating the transmitted forces to the vehicle body from road irregularities and to maintain vehicle controllability by keeping tire-road contact during various driving maneuvers. An ideal vehicle suspension system should have the capability to reduce the displacement and acceleration of the vehicle body for improvement of ride comfort. It should also aim to minimize the dynamic deflections of the tire to maintain tire-terrain contact to achieve a better vehicle handling and stability. Generally, a vehicle suspension design encounters conflicting requirements on ride comfort and handling. To cope with these problems, researches on vibration control using the SASS have increased significantly since these systems can provide performance benefits over passive suspensions and without requiring large power sources, multiple sensors, complex actuators and expensive hardware relative to the active suspensions.

Recently, the SASS using MR dampers have been studied by many researchers [1-6] because of their fast response characteristics to magnetic fields, insensitivity to temperature variations, obtainment of simple power and wide control bandwidth. The velocity of the fluid is controllable by the low input voltage or current to the MR damper without any external power source requirements. On the contrary, active suspension systems rely entirely on external power to operate the actuators and supply the control forces. In many applications, they need a large power source. There are two approaches to model the MR damper: nonparametric and parametric model. Choi et al. [7] developed a polynomial model, which can easily calculate the input current with measurable velocity and has been utilized in several semi-active control systems. A number of parametric models have been proposed to describe the force response of the damper.

The Bouc-Wen model is a popular approach for damper modeling because it includes hysteresis and a phenomenological approach to the yield characteristics of the damper fluid. Spencer et al. [8] designed a proper phenomenological model for such dampers based on the modified Bouc-Wen hysteresis model.

Regarding the review of previous studies, there is not considerable literature about tuning of the controller gains for the SASS based on frequency contents of road irregularities. However in this regard, a few papers [9-10] were found, introducing a new model-based estimation algorithm for real-time application to reconstruct the road roughness. To design the model-based adaptive observer, the vehicle needs to be described by a quarter of vehicle model while the road profile should be modeled by a finite number of sinusoidal waves with time varying characteristics in amplitude and frequency. Nguyen et al. [11] proposed a road-frequency adaptive control for SASS. The damping coefficients were scheduled according to the frequency regions of the road irregularities so that the SASS can improve the suspension performance in both vehicle handling and ride comfort. In the mentioned works, the road profile was considered as a composition of finite number of sinusoidal components. However, this cannot describe

* Corresponding Author:
E-mail address: ab_soltany@yahoo.com – Tel, (+98) 9127868977

Received: 05 August 2018; Accepted: 15 October 2018

effectively the high transient phenomena when the vehicle is exposed to a swept frequency input.

The performance of SASS with constant gains deteriorates when the road excitement frequencies are equal to the natural frequencies of the unsprung masses. This causes the resonance phenomena to occur and consequently, the vertical wheel acceleration to be more intense. In these circumstances, the SASS with constant gains cannot be considerably useful to enhance the ride comfort and road holding.

In this study, to cope with this problem, the SASS has been proposed based on two control strategies utilizing the ANFIS with variable gain. While one of them is considered for the enhancement of ride comfort, the other one is for the vehicle handling improvement. The scaling factor of ANFIS is tuned by PSD and WT methodologies.

2. System Dynamics Model

2.1. Quarter-car Suspension Model

In this work, a quarter-car suspension model is used for the controller design, as illustrated in Figure 1. The motion equations for the sprung and unsprung masses are given as

$$m_s\ddot{z}_s + c_s(\dot{z}_s - \dot{z}_u) + k_s(z_s - z_u) + F_{MR} = 0 \quad (1)$$

$$m_u\ddot{z}_u - c_s(\dot{z}_s - \dot{z}_u) - k_s(z_s - z_u) + k_t(z_u - z_r) - F_{MR} = 0 \quad (2)$$

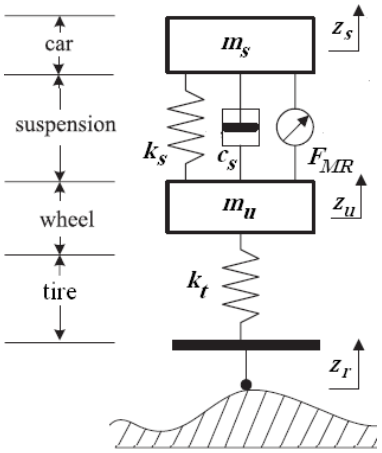

Figure 1. Quarter-car suspension model with MR damper

where, m_s is the sprung mass, which represents the car body; m_u is the unsprung mass, which represents the wheel assembly; c_s and k_s are damping and stiffness of the passive suspension, respectively, k_t is stiffness of the pneumatic tire. $Z_s(t)$ and $Z_u(t)$ are the displacements of the sprung and unsprung masses, respectively; $Z_r(t)$ is the road displacement input; F_{MR} represents the control force of the SASS, which is generated by the MR damper.

2.2. MR damper Modeling

There are several models for MR damper including Bingham model and Bouc-Wen model. In this article, a modified LuGre MR damper model is applied to generate the semi-active damping force F_{MR} by the input current, as shown in Figure 2. In addition, there are some kinds of MR fluids to apply for the dampers. In this study, the type of MR fluid is LORD MRF-132DG and an MR damper of the RD-1005-3 series manufactured by LORD Corporation is used [12]. The RD-1005-3 is a compact commercial MR damper that can be controlled by an input current which varies from 0–2 A and an input DC voltage of 12 V. The MRF-132DG fluid is a hydrocarbon-based MR fluid formulated for general use in controllable and energy-dissipating applications such as shock absorbers, dampers and brakes. The model of the MR damper is expressed as follows, [13-14]

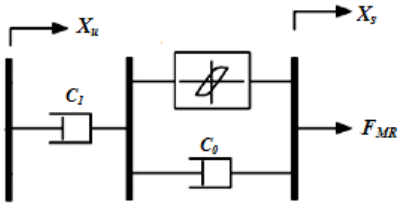

Figure 2. Modified LuGre model for the MR damper

$$F_{MR} = (\alpha_a + \alpha_b v)z + (c_{0a} + c_{0b}v)\dot{x} + c_1\dot{z} \quad (3)$$

$$\dot{z} = \dot{x} - a_0|\dot{x}|z \quad (4)$$

$$x = x_s - x_u \quad (5)$$

$$v = 2.406i + 0.435 \quad (6)$$

where, z is the hysteresis variable, α_a is the stiffness of z, α_b is the stiffness of z influenced by voltage v, i represents the circulating current in the damper coil. c_{0a} is the viscous damping coefficient, c_{0b} is the damping coefficient influenced by v, c_1 is the damping coefficient of z, x represents the wheel travel, and a_0 is a constant value. These parameters are set as $\alpha_a = 15\ KN/m$, $\alpha_b = 40\ KN/mV$, $c_{0a} = 100\ Ns/m$, $c_{0b} = 2500\ Ns/mV$, $c_1 = 200\ Ns/m$ and $\alpha_0 = 190$ [13]. The simulated damping forces are depicted in Figure 3, where the sinusoidal excitation frequency and amplitude of x are 2.5 Hz and 5 mm, respectively. The applied input currents are 0.25, 0.5 and 1 A.

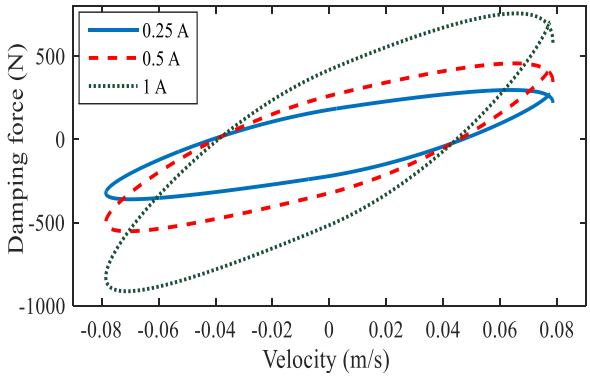

Figure 3. Relationship between MR damper forces versus velocity

3. Semi-active Control System Design

In this research, the SASS is proposed to enhance the vehicle handling and ride comfort based on two approaches. SAS1 is for enhancement of the ride comfort and SAS2 is for improvement of the road holding.

3.1. Ride Comfort (SAS1)

In this part, a fuzzy controller has been used to improve the ride comfort. The control inputs are the sprung mass velocity $\dot{z}_s$ and the relative velocity between the sprung and unsprung mass ($\dot{z}_{su} = \dot{z}_s - \dot{z}_u$). The MR damper force is taken into account as control output. The relative velocity $\dot{z}_{su}$ is defined to be positive when damper is separating. Seven linguistic variables and easily calculated triangle membership functions are selected for both the input and output. Table 1 shows the fuzzy rules of the ride comfort strategy, where, NB, NM, NS, ZE, PS, PM, PB represent 'negative big', 'negative medium', 'negative small', 'zero', positive small', positive medium' and 'positive big', respectively. Based on Table 1, a Mamdani method is employed in the fuzzy reasoning, whereas max-min inference method is chosen as aggregation operator, and defuzzification is performed using the centre-average method [13]. In practical applications, the control input to the MR damper can be bounded as *sat (f (t))*, where its saturation function of control input *f (t)* is expressed as

$$Sat(f(t)) = \begin{cases} -1300\ N & if\ f(t) < -1300 \\ f(t) & if\ -1300 \le f(t) \le 1300 \\ 1300\ N & if\ f(t) > 1300 \end{cases} \quad (7)$$

The control input applied to the MR damper has the following semi-active condition imposed

$$f(t) = \begin{cases} f(t) & if\ \ f(t)\,\dot{z}_{su} < 0 \\ 0 & if\ \ f(t)\,\dot{z}_{su} \ge 0 \end{cases} \quad (8)$$

Table 1. The rule base of fuzzy control for the SAS1

	Relative velocity $\dot{z}_{su}$						
$\dot{z}_s$	NB	NM	NS	ZE	PS	PM	PB
NB	PB	PB	PM	PS	ZE	ZE	ZE
NM	PB	PM	PM	PS	ZE	ZE	ZE
NS	PM	PM	PS	ZE	ZE	ZE	ZE
ZE	PS	PS	ZE	ZE	ZE	NS	NS
PS	ZE	ZE	ZE	ZE	NS	NM	NM
PM	ZE	ZE	ZE	NS	NM	NM	NB
PB	ZE	ZE	ZE	NS	NM	NB	NB

An important index for the evaluation of ride comfort is the root mean square (RMS) value of the vertical sprung mass acceleration defined as

$$RMS(\ddot{z}_s) = \sqrt{\frac{1}{T}\int_0^T \ddot{z}_s^2\ dt} \quad (9)$$

3.2. Road Holding (SAS2)

In this section, first, a fuzzy controller is designed to improve the vehicle road holding. Then, an ANFIS control structure is built based on the proposed fuzzy system. Table 2 illustrates the fuzzy rules of the SAS2 system [13]. In the fuzzy system, the input current to the MR damper is considered as the control output and its range is [0, 1] *A*. To build the ANFIS, five generalized bell-shaped membership functions are selected for both the input and output, and hybrid algorithm is chosen for optimization process. The number of iterations is set to 40.

Table 2. The rule base of fuzzy control for the SAS2

	Relative velocity $\dot{z}_{su}$						
$\dot{z}_s$	NB	NM	NS	ZE	PS	PM	PB
NB	B	B	B	B	ZE	ZE	ZE
NS	B	B	M	M	ZE	ZE	ZE
ZE	B	M	M	S	ZE	S	S
PS	M	S	S	S	S	S	M
PM	S	S	S	ZE	S	S	B
PB	ZE	ZE	ZE	ZE	S	M	B

The performance index for the aluation of vehicle handling and road holding is the RMS value of the tire deflection, RMS(Td), expressed as

$$RMS(Td) = \sqrt{\frac{1}{T}\int_0^T (z_u - z_r)^2\ dt} \quad (10)$$

By minimising the RMS value of tyre deflection, the variations of normal tyre forces are reduced. This decreases the variations of lateral and longitudinal tyre forces, and then the improvement of vehicle handling and road holding is achieved. The tyre deflection depends on the frequency contents of road profile and the resonance phenomena. The reduction of resonance effect can be achieved by revealing the frequency contents of road irregularities. In this study, this is performed through the WT and PSD methods. WT is described in the next section.

3.3. Wavelet Transform (WT)

Wavelet transform is divided into two parts: continuous wavelet transform (CWT) and discrete wavelet transform (DWT). The CWT is based upon a family of functions, [15]

$$\psi_{a,b}(t) = \frac{1}{\sqrt{a}}\psi\left(\frac{t-b}{a}\right),\ \ a > b \in \mathcal{R} \quad (11)$$

where, ψ is a fixed function, called the 'mother wavelet', which is localized both in time and frequency. The function $\psi_{a,b}(t)$ is obtained by applying the operations of shifting b in the time domain and scaling a in the frequency domain to the mother wavelet. In this work, the Symlet wavelet is employed using MATLAB software, in which f_o=*0.667* Hz is used throughout the mother transformations (f_o is the central frequency of the wavelet). The CWT of a signal x(t) is given by

$$W_x^{\psi}(a,b) = \int_{-\infty}^{\infty} x(t)\psi_{a,b}^{\star}(t)dt = \frac{1}{\sqrt{a}}\int_{-\infty}^{\infty} x(t)\psi^{\star}\left(\frac{t-b}{a}\right)dt \quad (12)$$

where, $\psi^{\star}(t)$ is the complex conjugate of $\psi(t)$. The relationship between the scale parameter *a* and frequency f_a can be obtained as, [15]

$$f_a = \frac{f_o}{a\,\Delta} \quad (13)$$

where, f_a is the frequency corresponding to the scale *a*, in Hz, and Δ is the sampling frequency.

The signal energy in the scale *a*, and the translation b, is expressed as

$$E(a,b) = \left|W_x^{\psi}(a,b)\right|^2 \quad (14)$$

The total signal energy distribution at scale *a* is given by

$$E(a) = \int_{-\infty}^{\infty} E(a,b)db \quad (15)$$

The square of the modulus of the CWT can be interpreted as an energy density distribution over the *(a,b)* time-scale plane. As mentioned earlier, the DWT is the other type of WT. The DWT can be derived from the CWT. The most obvious difference is that the DWT utilizes scale and position values based on powers of two. The values of a and b are: $a = 2^j$, b = k ×2j and (j, k)∈Z^2, where j is level of decomposition. So, the Eq. (11) is rewritten as

$$\psi_{j,k}(n) = 2^{-0.5j}\,\psi(2^{-j}n - k), \quad (j,k) \in Z^2 \quad (16)$$

and, the DWT coefficients of discrete signal x(n) is calculated by

$$C(j,k) = \sum_{n \in Z} x(n)\,\psi_{j,k}(n) \quad (17)$$

The levels of 1, 2 and 3 for the DWT are corresponding to scales of 2, 4 and 8 for the CWT, respectively. In this work, a combined use of the ANFIS and the WT is presented to obtain the input current to control the MR damper. First, the DWT vertical wheel acceleration is controlled, thereafter; the energy of acceleration signal is determined at level of 5 by Eq. (15). The level is chosen according to Eq. (13).

$$if\ level = 5 \xrightarrow{yields} f_a = \frac{0.667}{2^5 \times 0.002} = 10.4\ Hz \quad (18)$$

The level of 5 is a proper selection, because the natural frequency value of the unsprung mass usually ranges from 8 to 12 Hz. After computing the energy of acceleration signal and using a linear relationship between the energy and the scaling factor of control input for the ANFIS, the factor is updated online.

4. Simulation Results

In order to evaluate the effectiveness of the proposed controller, a quarter-car suspension model is considered for the simulation. The model parameters are shown in Table 3. The simulations are conducted in the MATLAB software and the data sampling frequency is 500 Hz. This means the sampling period is 0.002 s.

Table 3. Parameter values of the quarter-car suspension model

Parameter	value
Sprung mass, m_s (Kg)	300
Unsprung mass, m_u (Kg)	30
Suspension stiffness, k_s (N/m)	16800
Tyre stiffness, k_t (N/m)	168000
Suspension damping coefficient, c_s (N.s/m)	1300

4.1. Ride Comfort Investigation

According to the international directive ISO 8608 typical road profiles can be grouped into classes from A to E which can be employed to analyze the roughness of various roads from very smooth highways to rather rough roads covered with pebbles, respectively. In this part, it is presumed that the vehicle runs on a road with medium roughness quality and small pebbles classified as type C, [16], and illustrated in Figure 4. The ride comfort in the vertical direction becomes the main control target.

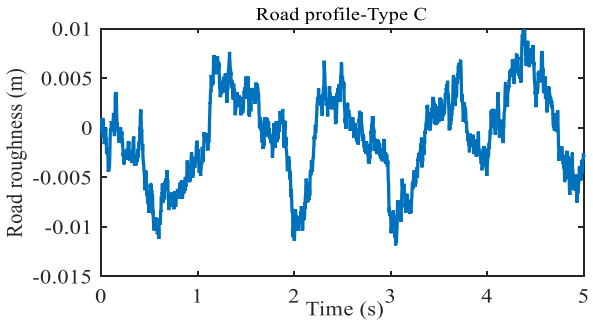

Figure 4. A typical random road profile of class C

Therefore, the SAS1 will act under the mentioned conditions. The vertical displacement and acceleration of unsprung mass are plotted in Figures 5 and 6, respectively.

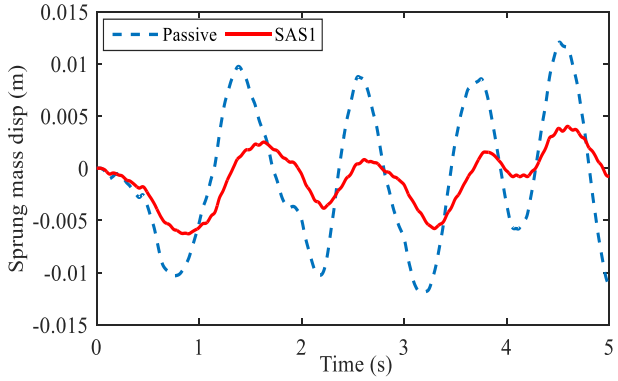

Figure 5. Vertical displacement of the sprung mass

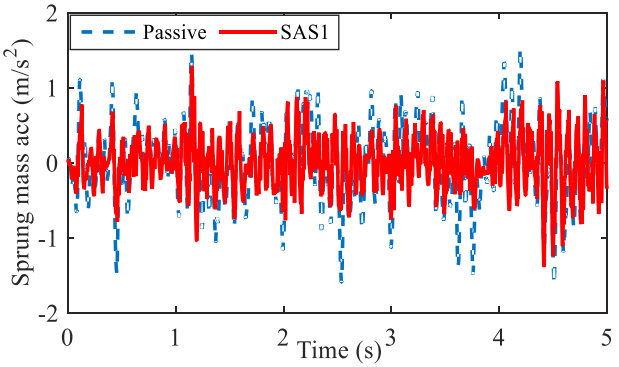

Figure 6. Vertical acceleration of the sprung mass

It can be observed that the displacement and acceleration of car body for the SAS1 are reduced significantly compared with the passive vehicle. The RMS value of acceleration signal is used to evaluate the SAS1 performance. The calculated RMS values of the passive and the SAS1 systems are 0.521 and 0.364, respectively. Therefore, the SAS1 has reduced the RMS by about 30%. The simulation results show that the designed SASS can improve the ride comfort considerably compared with the passive vehicle.

The applied input current of MR damper and the control force of SAS1 are also shown in Figures 7 and 8, respectively.

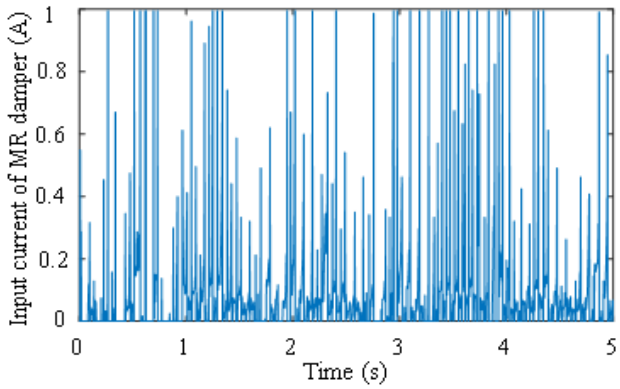

Figure 7. Input current to the MR damper

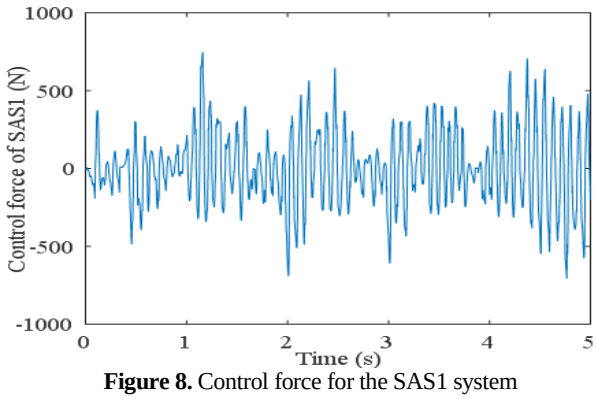

Figure 8. Control force for the SAS1 system

4.2. Road Holding Investigation

In this section, the scaling factor of control input current for the ANFIS is updated online via the WT and the PSD methods when the wheel is excited by the inputs, including transient characteristics like the swept frequency signal. In order to evaluate of WT effectiveness, it is not necessarily required to analyze the transient signals in a long time. Thus, the simulation time is considered to be equal to 2s. The road excitation is C-class road surface, in which, a swept frequency input with amplitude of 8 mm and frequency region of [8, 12] Hz is added for an interval of 0.5s between 0.5 to 1s, as depicted in Figure 9. In order to assess the performance of proposed control algorithm, the tire deflection signal is evaluated for three systems, as illustrated in Figure 10(a), the passive system, the SAS2 system which uses the ANFIS and the PSD methods (ANFIS with PSD) and the SAS2 system that utilizes the ANFIS and the WT methods (ANFIS with WT). By zooming in between 0.5 to 1s on this diagram, the changes of curves are observed obviously in Figure 10(b). In addition, the RMS values of tire deflection for the systems are computed, as given in Table 4.

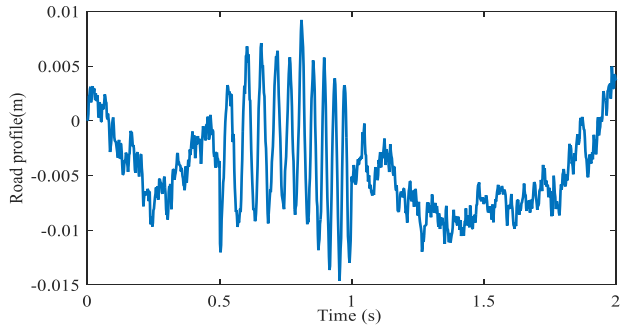

Figure 9. A random road roughness combined with a swept frequency input

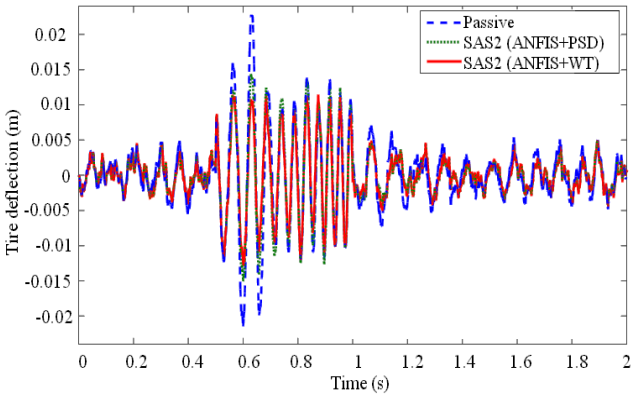

(a)

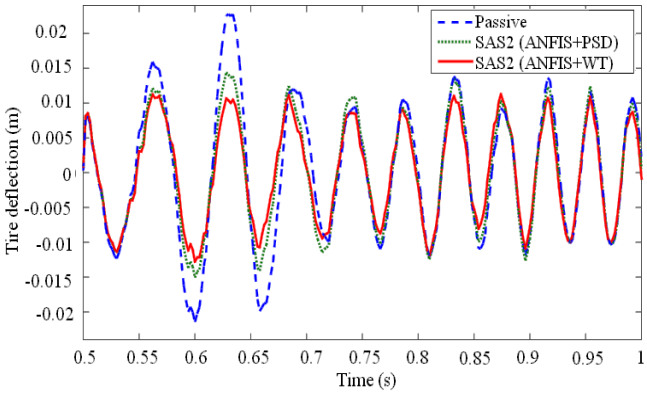

(b)

Figure 10. Tire deflection: (a) total interval; (b) zoom in between 0.5 to 1s

Table 4. Comparison between the RMS of tyre deflection for different suspension systems

Interval (s)	RMS (mm)		
	Passive	SAS2 (ANFIS+PSD)	SAS2 ANFIS+WT)
[0, 0.5]	2.2	1.8	1.8
[0.5, 1]	9.9	8.2	7.1
[1, 1.5]	3	2.1	2
[1.5, 2]	2.3	1.8	1.8
Total Interval	5.4	4.4	3.9

According to Table 4, it can be concluded that both the controller systems, ANFIS with PSD and ANFIS with WT, have the same results to decrease the RMS of tire deflection for the first and the fourth intervals. Hence, the vehicle road holding can be improved. The reason is that the road irregularities do not have high transient specifications in these spans. However, the frequencies of road input are time-variant in the second interval, thus the system is subjected to severe transient characteristics. In this condition, the ANFIS controller combined with WT has better performance compared with the ANFIS with PSD algorithm. In comparison to the passive system, the RMS values of tire deflection are reduced through these two controller systems by 28.3% and 17.3%, respectively. There were also a few differences for the results of two controller structures in the third interval. In comparison to the other controller, the ANFIS with WT controller reduces the RMS value by 3.3%. This is due to the existence of the insignificant transient specifications in the system response for the time span. The input current of MR damper and the control force for the SAS2 system by using two proposed controllers are seen in Figures 11 and 12, respectively.

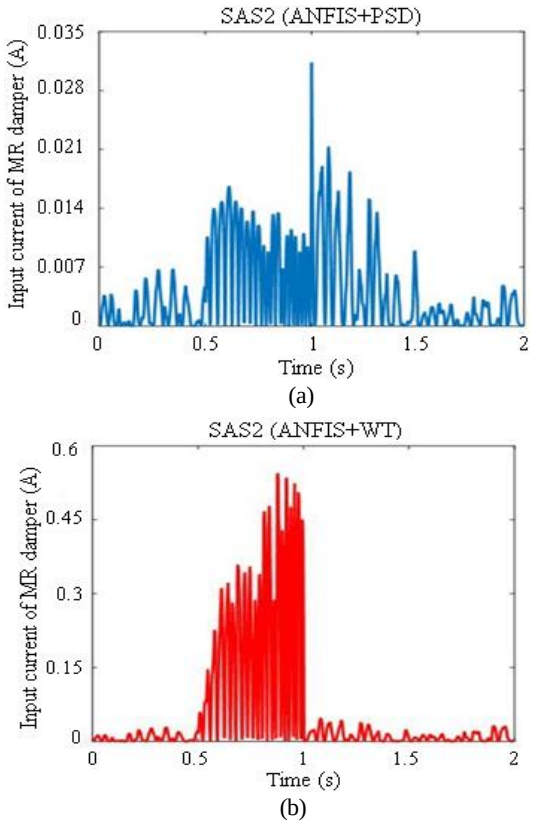

Figure 11. Input current to the MR damper: (a) ANFIS with PSD controller, (b) ANFIS with WT controller

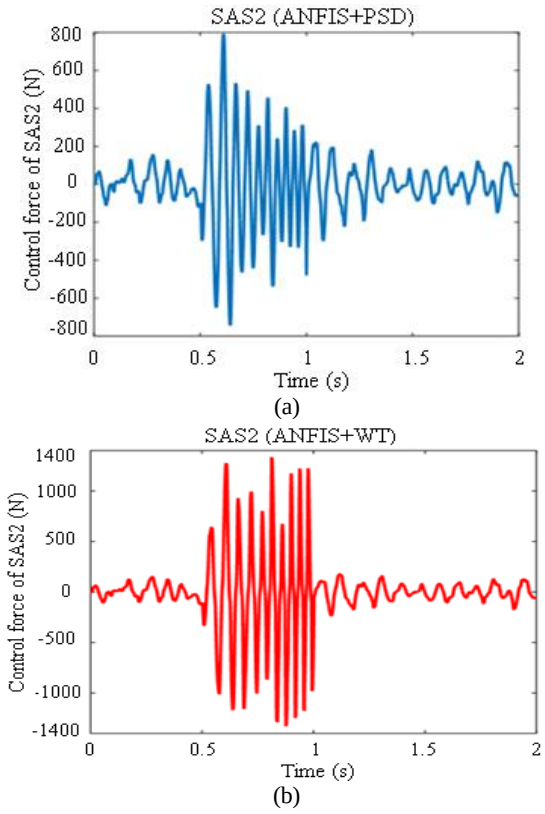

Figure 12. Control force for the SAS2 system: (a) ANFIS with PSD controller, (b) ANFIS with WT controller

5. Conclusions

In this paper, a new controller for the SASS featuring MR damper was proposed based on the ANFIS focusing on the enhancement of the ride comfort, road holding and vehicle handling. A quarter-car suspension model with two degrees of freedom that consists of sprung and unsprung masses was utilized for the controller design. When the frequency contents of road excitation are equal to the natural frequency of the wheel, the resonance phenomena occurs, which causes severe oscillations revealed on vertical wheel motion. In this circumstance, the conventional SASS based on ANFIS with constant gains cannot be very useful. In order to overcome this problem, the scaling factor of control input current for the ANFIS was adjusted by adopting the WT and the PSD methods.

The road input was considered as a random road roughness combined with a swept frequency signal to excite the natural frequency of the unsprung mass. Simulation results on the random road profile with high transient phenomena demonstrated that the ANFIS with WT controller can be more adaptable in comparison to the ANFIS with PSD controller. It was found that the first controller decreased the RMS values of tire deflection by 28.3%, whereas the second controller reduced the same variable by about 17.3%. However, the both controllers had the same results to reduce the RMS of tire deflection when the road irregularities do not have high transient characteristics. Therefore, it can be concluded that the ANFIS with the WT is more proper technique compared with the PSD analysis to update the gains of the SASS. This advantage improved the road holding whenever the resonance of vertical wheel motion is probable. This is the main technical contribution of this research work.

It is finally noted that the ANFIS controller associated with the PSD and WT proposed in this work can be implemented to a full-car suspension model without any significant modification.

Nomenclature

c_s	: suspension damping coefficient
F_{MR}	: control force of the MR damper
k_s	: suspension stiffness
k_t	: tire stiffness
m_s , m_u	: sprung mass and unsprung mass
z_r	: road excitation
z_s	: vertical displacement of the sprung mass
z_u	: vertical displacement of the unsprung mass

References

[1] S.B. Choi, H.S. Lee, Y.P. Park, H_∞ control performance of a full-vehicle suspension featuring magnetorheological dampers, Vehicle System Dynamics 38 (2002) 341–360.

[2] M.Yu, X.M. Dong, S.B. Choi, C.R. Liao, Human simulated intelligent control of vehicle suspension with MR dampers, Journal of Sound and Vibration 319 (2009) 753–767.

[3] S.D. Nguyen, S.B. Choi, Q.H. Nguyen, A new fuzzy-disturbance observer-enhanced sliding controller for vibration control of a train-car suspension with magnetorheological dampers, Mechanical Systems and Signal Processing 105 (2018) 447–466.

[4] S.D. Nguyen, Q.H. Nguyen, S.B. Choi, A hybrid clustering based fuzzy structure for vibration control-Part 2: An

application to semi-active vehicle seat-suspension system dampers, Mechanical Systems and Signal Processing 56-57 (2015) 288–301.

[5] D.X. Phu, S.M. Choi, S.B. Choi, A new adaptive hybrid controller for vibration control of a vehicle seat suspension featuring MR damper, Journal of Vibration and Control 23 (2017) 3392–3413.

[6] D.X. Phu, N.Q. Hung, S.B. Choi, A novel adaptive controller featuring inversely fuzzified values with application to vibration control of magneto-rheological seat suspension system, Journal of Vibration and Control 24 (2017) 5000–5018.

[7] S.B. Choi, S.K. Lee, Y.P. Park, A hysteresis model for the field-dependent damping force of a magnetorheological damper, Journal of Sound and Vibration 245 (2001) 375–383.

[8] B.F. Spencer, S.J. Dyke, M.K. Sain, J.D. Carlson, Phenomenological Model for Magneto-rheological Dampers, Journal of Engineering Mechanics 123 (1997) 230–238.

[9] M. Doumiati, O. Sename, M.K. Sain, J.D. Carlson, L. Dugard, D. Lechner, Road profile estimation using an adaptive Youla-Kucera parametric observer: Comparison to real profilers, Control Engineering Practice 61 (2017) 270–278.

[10] J.C.T. Martinez, S. Fergani, O. Sename, J.D. Carlson, L. Dugard, D. Lechner, Adaptive road profile estimation in semiactive car suspension, IEEE Transactions on Control Systems Technology 23 (2015) 2293–2305.

[11] L.H. Nguyen, K. Hong, S. Park, Road-frequency adaptive control for semi-active suspension systems, Journal of Control, Automation, and Systems 8 (2010) 1029–1038.

[12] LORD Corporation, https://www.lord.com

[13] A. Soltani, A. Bagheri, S. Azadi, Integrated vehicle dynamics control using semi-active suspension and active braking systems, Proc. IMechE, part K: Journal of Multi-body Dynamics 232 (2017) 314–329.

[14] R. Jimenez, L. Alvarez-Icaza, LuGre friction model for a magnetorheological damper, Structural Control and Health Monitoring 12 (2005) 91–116.

[15] S. Azadi, A. Soltani, Fault detection of vehicle suspension system using wavelet analysis, Vehicle System Dynamics 47 (2009) 403–418.

[16] G. Verros, S. Natsiavas, C. Papadimitriou, Design optimization of quarter-car models with passive and semi-active suspension under random road excitation, Journal of Vibration and Control 11 (2005) 581–606.